iScience, Volume *25*

Supplemental information

Multimodal imaging of the dynamic brain tumor microenvironment during glioblastoma progression and in response to treatment

Anoek Zomer, Davide Croci, Joanna Kowal, Leon van Gurp, and Johanna A. Joyce

Supplemental Information

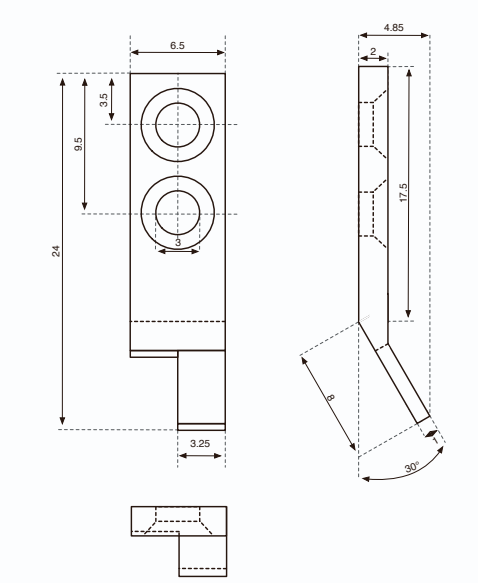

Figure S1. Head-bar schematic, related to Figure 1. Head bars were made from polyether ether ketone (PEEK) and were produced by 3D printing. Metric unit: mm.

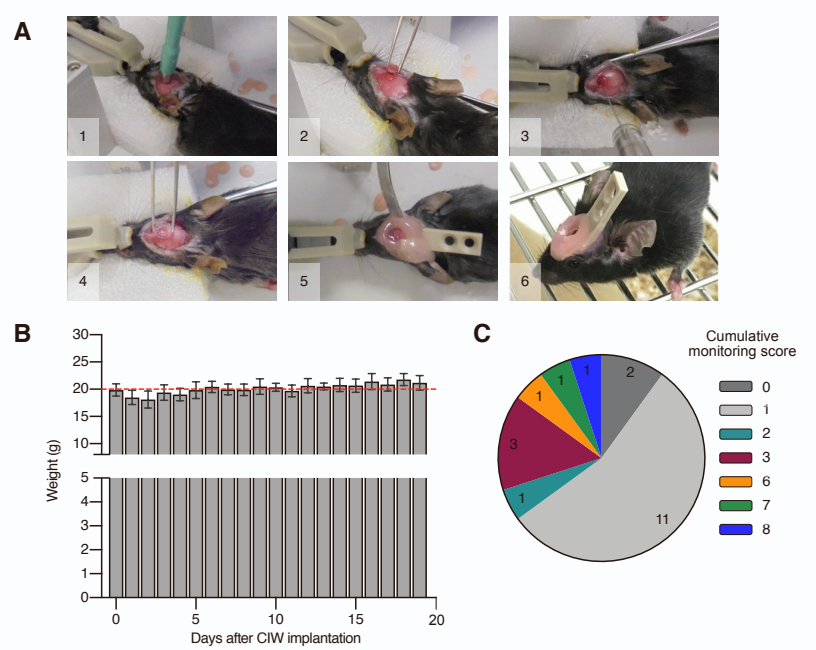

Figure S2. Mice show a rapid and full recovery after CIW implantation, related to Figure 1. (A) Fully anaesthetized mice were placed on a heated stereotactic frame. A 3 mm biopsy punch was used to remove a circular fragment of the skull (images 1 and 2). DF1 virus-producing cells were then injected with a high-precision Hamilton's syringe (image 3) to subsequently induce tumor formation over time. Afterwards, the skull was closed by applying the cranial imaging window, which was fixed with super-glue and dental cement. Simultaneously, a head-bar was placed (images 4 and 5) which allowed the stabilization of the mouse's head during subsequent two-photon microscopy experiments and avoided breathing-associated movements. The mouse was then returned to the cage and monitored while recovering from the surgery and anesthesia (image 6). (B) Monitoring of mouse weight following surgery (n=20 mice), showing a rapid recovery of body weight. The dashed red line shows the mean weight on the day of surgery. Data are represented as mean ± SD. (C) Evaluation of the overall mouse welfare 2 days post-surgery (see STAR Methods for a detailed description of the monitoring scoring system). The numbers in each sector of the pie chart correspond to the number of mice in that particular category.

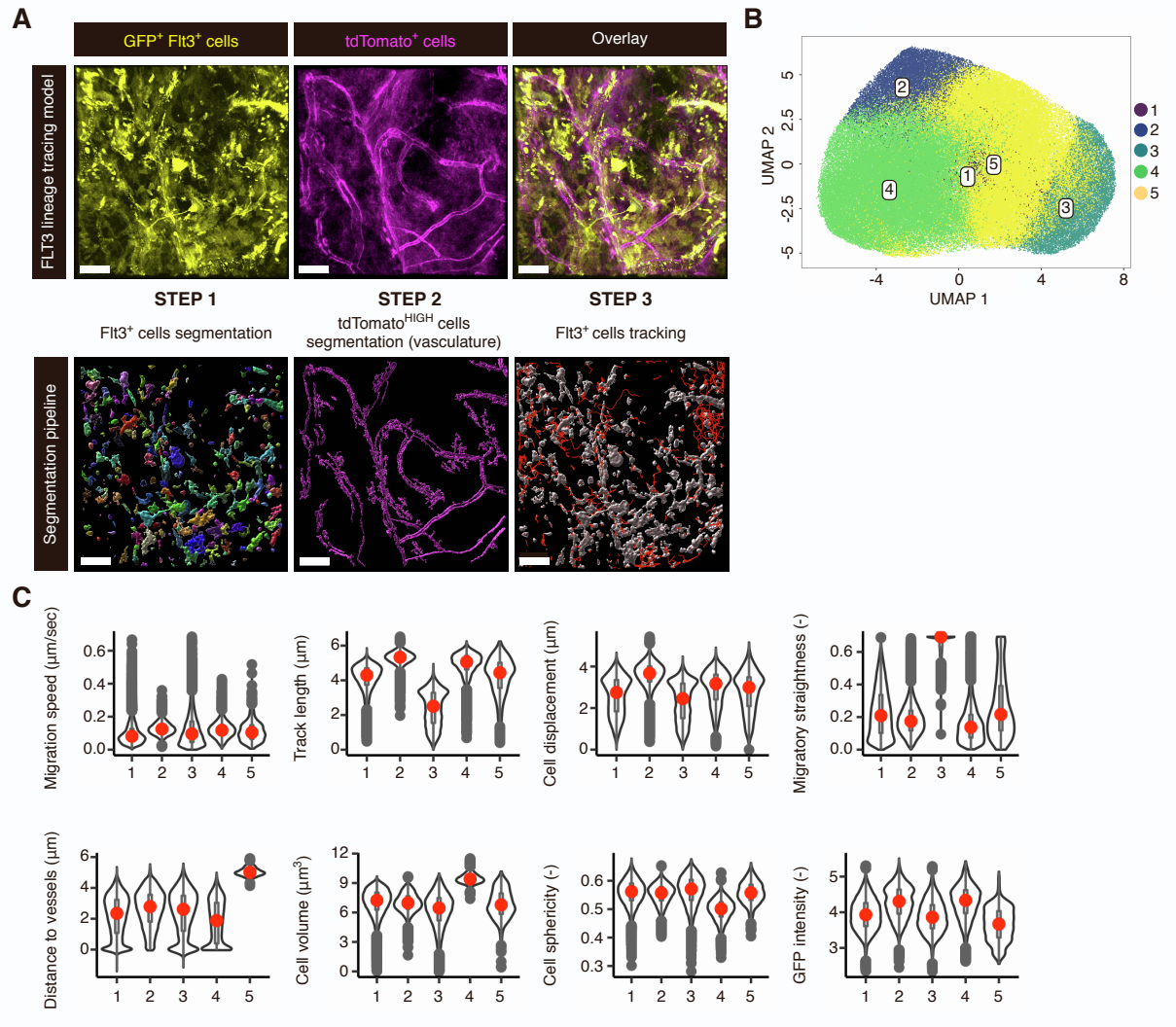

Figure S3. Dimensionality reduction analysis reveals distinct cell clusters in the FLT3 lineage-tracing model, related to Figure 4. (A) Segmentation and migration analysis of the FLT3 lineage-tracing model. GFP$^+$Flt3$^+$ or tdTomato$^+$ cells (upper panel) were segmented in order to identify Flt3$^+$ peripheral immune cells (step 1) and highly tdTomato-expressing cells highlighted the vasculature (step 2). Flt3$^+$ cell migration was tracked as the final step (step 3). (B) UMAP visualization of Flt3$^+$ cell clusters. 93 time-lapses were analyzed, for a total of 135,100 Flt3$^+$ cells (*Ink4a/Arf*-deficient model n=9 mice, *p53*-deficient model n=5 mice). (C) Violin plots showing the different cell features in each of the clusters (the cluster numbers correspond to the IDs shown in (A)). The red dot on each violin plot represents the median. Y-axis are displayed as logarithmic scale.

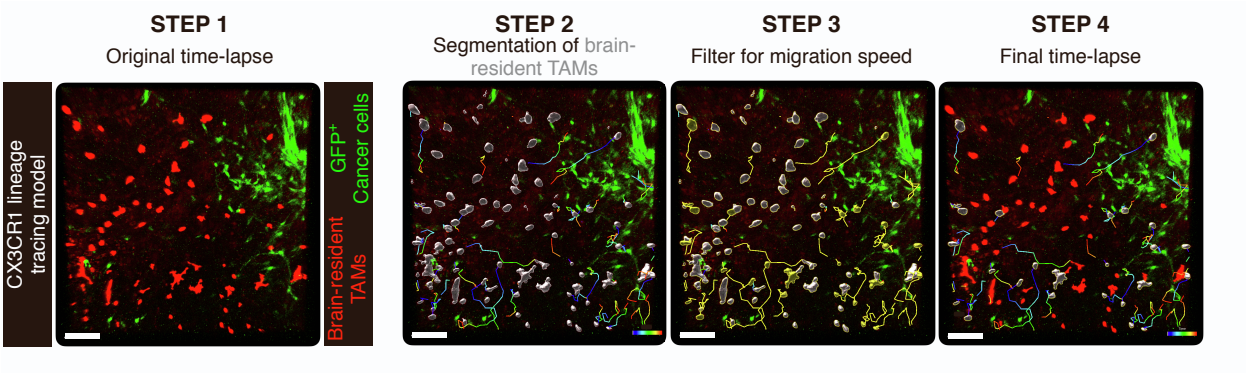

Figure S4. Filtering of migrating brain-resident TAMs, related to Figure 4. Cells were segmented and their movement was tracked over the entire course of the time-lapse (steps 1 and 2). Subsequently, cell speed was used to discriminate migratory cells from stationary cells (yellow lines, track speed ≥ 0.05 μm/s, steps 3 and 4). Scale bars: 100 μm. Color-coded tracks display time through the time-lapse (blue indicates the start, and red indicates the end of the imaging acquisition).

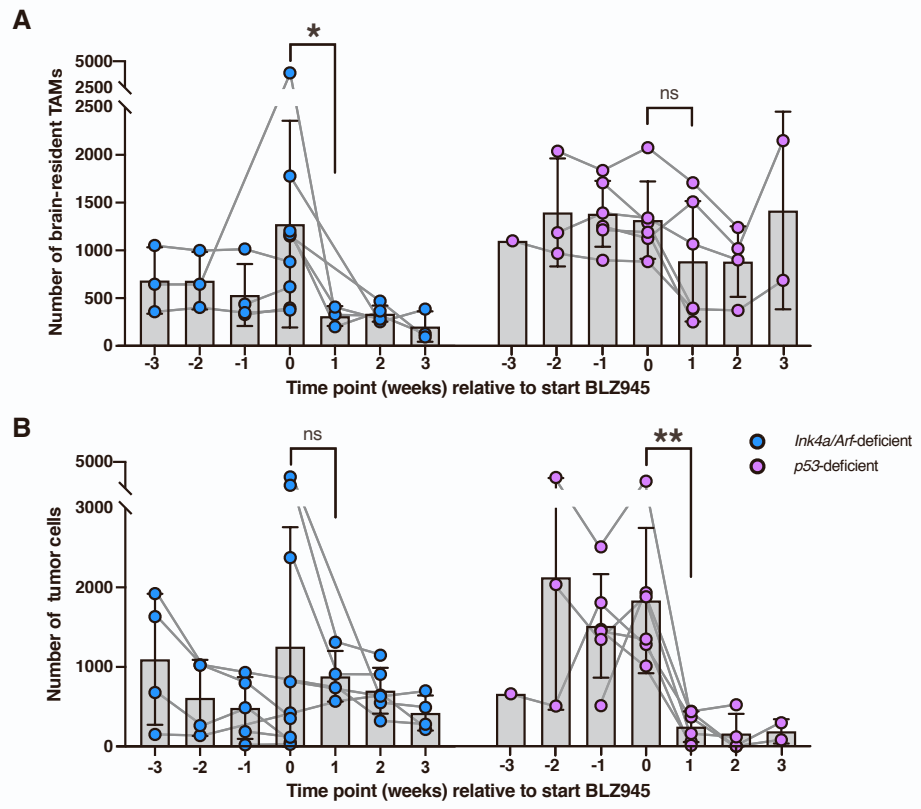

Figure S5. Dynamics of brain-resident TAMs and tumor cells during glioblastoma progression and in response to BLZ945 treatment, related to Figure 4. (A) Quantification of the number of brain-resident TAMs and (B) tumor cells, in both *Ink4a/Arf*-deficient and *p53*-deficient GBMs. Each dot represents the number of cells in one FOV (Student's t-test, ns: not significant, * indicates P<0.05, and ** indicates P<0.01). Data are represented as mean ± SD.

Table S1. List of antibodies used, related to Figure 2 and 3.

Antibodies							
Target	**Species**	**Antibody**	**Manufacturer**	**Clone**	**Category number**	**Dilution**	**Application**
Ly-6C	Rat	Anti-mouse Ly-6C Brilliant Violet 711	BioLegend	HK1.4	128037	1:800	Flow cytometry panel #1
Ly-6G	Rat	Anti-mouse Ly-6G Brilliant Violet 605	BioLegend	1A8	127639	1:160	Flow cytometry panel #1
CD11b	Rat	Anti-mouse CD11b BUV661	BD Biosciences	M1/70	612977	1:800	Flow cytometry panel #1, Flow cytometry panel #2
CD49d	Rat	Anti-mouse CD49d PE/Cy7	BioLegend	R1-2	103618	1:160	Flow cytometry panel #1
CD45	Rat	Anti-mouse CD45 Alexa Fluor 700	BioLegend	30-F11	103128	1:200	Flow cytometry panel #1, Flow cytometry panel #2
CD3	Hamster	Anti-mouse CD3e BUV395	BD Biosciences	145-2C11	563565	1:75	Flow cytometry panel #1 and #2
NK-1.1	Mouse	Anti-mouse NK-1.1 Brilliant Violet 421	BioLegend	PK136	108741	1:640	Flow cytometry panel #1
CD19	Rat	Anti-mouse CD19 Brilliant Violet 605	BioLegend	6D5	115539	1:320	Flow cytometry panel #2
NK-1.1	Mouse	Anti-mouse NK-1.1 Brilliant Violet 711	BioLegend	PK136	108745	1:640	Flow cytometry panel #2
Collagen I	Rabbit	Anti-mouse collagen I	Abcam	Polyclonal	ab34710	1:100	Immunofluorescence panel #1
YFP	Chicken	Anti-GFP (cross-reactive to YFP)	Abcam	Polyclonal	ab13970	1:1000	Immunofluorescence panel #1
Chicken IgG (H+L)	Donkey	Anti-chicken IgG Alexa Fluor 488	Jackson ImmunoResearch	Polyclonal	703-545-155	1:500	Immunofluorescence panel #1
Rabbit IgG (H+L)	Donkey	Anti-rabbit IgG Alexa Fluor 647	Invitrogen	Polyclonal	A31573	1:500	Immunofluorescence panel #1

Flow cytometry panels #1 and #2 have been used in experiments presented in Figure 2.

Immunofluorescence panel #1 has been used in experiments presented in Figure 3.